Journal of Physics: Conference Series **2446** (2023) 012018 doi:10.1088/1742-6596/2446/1/012018

Search for $K^0 \to \mu^+\mu^-\mu^+\mu^-$ at the LHCb experiment

Miguel Fernández Gómez, on behalf of the LHCb collaboration.

Instituto Galego de Física de Altas Enerxías (IGFAE), Rúa de Xoaquín Díaz de Rábago, 15705 Santiago de Compostela, Spain

E-mail: miguel.fernandez.gomez@cern.ch

Abstract. These proceedings discuss the search for $K^0_{S(L)} \to \mu^+\mu^-\mu^+\mu^-$ decays, performed using proton-proton collision data collected by the LHCb experiment at a centre-of-mass energy of 13 TeV, corresponding to an integrated luminosity of $5.1\,\text{fb}^{-1}$. Upper limits are computed to be, at 90% C.L., $\mathcal{B}(K^0_{S(L)} \to \mu^+\mu^-\mu^+\mu^-) < 5.1 \times 10^{-12}$ (2.3×10^{-9}).

1. Introduction

The $K^0_S \to \mu^+\mu^-\mu^+\mu^-$ decay is a flavour-changing neutral current process that has not yet been observed. In the Standard Model (SM), its highly-suppressed decay rate is predicted to be [1]:

$$\mathcal{B}(K^0_S \to \mu^+\mu^-\mu^+\mu^-)_{SM} \sim (1-4) \times 10^{-14}. \quad (1)$$

Similarly, $K^0_L \to \mu^+\mu^-\mu^+\mu^-$ is predicted in the SM to occur with a branching ratio of

$$\mathcal{B}(K^0_L \to \mu^+\mu^-\mu^+\mu^-)_{SM} \sim (4-9) \times 10^{-13}. \quad (2)$$

Physics beyond the SM (BSM) can lead to large enhancements of these values; for instance, proposed dark-sector scenarios like the $U(1)_d + S$ dark photons model, predict these branching fractions going up to $\sim 2 \times 10^{-12}$ and 2.5×10^{-10}, respectively [2, 3]. Additionally, an eventual measurement of the time interference between $K^0_S \to \mu^+\mu^-\mu^+\mu^-$ and $K^0_L \to \mu^+\mu^-\mu^+\mu^-$ could allow to determine the sign of $\mathcal{A}(K^0_L \to \gamma\gamma)$ [1].

The first-ever experimental search of these two decays is presented in these proceedings. The analysis used pp collision data collected by the LHCb experiment from 2016–2018 at a centre-of-mass energy of 13 TeV, corresponding to an integrated luminosity of $5.1\,\text{fb}^{-1}$. It follows the strategy set by the $K^0_S \to \mu^+\mu^-$ analyses by the LHCb collaboration [4, 5], measuring $\mathcal{B}(K^0_S \to \mu^+\mu^-\mu^+\mu^-)$ and $\mathcal{B}(K^0_L \to \mu^+\mu^-\mu^+\mu^-)$ relative to $\mathcal{B}(K^0_S \to \pi^+\pi^-)$.

2. The LHCb detector and trigger

The LHCb detector [6, 7] (see Fig. 1) is a single-arm forward spectrometer covering the pseudorapidity range $2 < \eta < 5$, designed for the study of particles containing b or c quarks. The pp collisions occur inside the vertex locator (VELO) [8], at a point referred to as the primary vertex (PV). The VELO is a high-precision tracking system that allows to differentiate between the primary and secondary vertices, and where around 22% of the K^0_S that are produced, decay [5]. After the VELO, the particles hit the first Ring imaging Cherenkov detector (RICH-1) [9], which allows for particle identification of low-momentum tracks. Tracking stations to

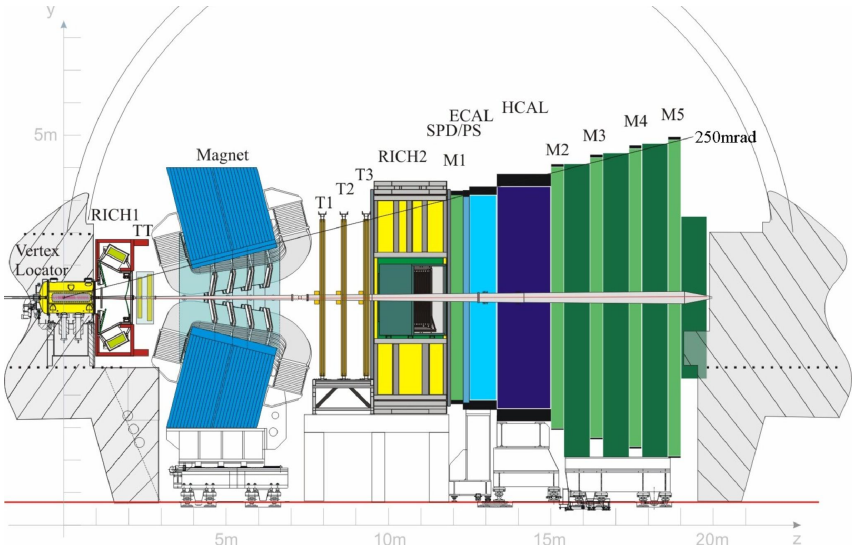

Figure 1. Side view of the LHCb detector layout [6].

reconstruct the trajectories and measure the momenta of charged particles, are located before (one station) and after (three stations) a dipole magnet [10]. A second RICH detector, RICH-2, is located right after the second group of tracking stations, allowing for particle identification of high-momentum tracks. A calorimeter system then identifies and measures the energy of photons, electrons and hadrons. Muons are identified by information collected by specialised chambers [11], as well as information from the tracking system, the calorimeter system, and the RICH detectors. The LHCb detector accumulated data in two Runs: Run 1 (2011–2012) and Run 2 (2015–2018).

Events are first required to pass a hardware-trigger selection, known as L0 [12], based on information from the calorimeter and the muon system, selecting p_{T} signatures above a few GeV/c. Subsequently, a full event reconstruction is applied in a two-step software selection, the High Level Trigger (HLT). Two trigger categories are defined in the LHCb analyses, based on whether particles independent of the signal decay trigger the event to be saved (TIS, triggered independent of signal) or the signal decay products do (TOS, triggered on signal). In the case of $K^0_{\mathrm{S(L)}} \to \mu^+\mu^-\mu^+\mu^-$, the sample is split into two categories according to the hardware trigger decision: one where an object in the event other than the muons from the $K^0_{\mathrm{S(L)}} \to \mu^+\mu^-\mu^+\mu^-$ selected candidate satisfy the L0 trigger selection (TIS), and another where the muons from $K^0_{\mathrm{S(L)}} \to \mu^+\mu^-\mu^+\mu^-$ selected candidates are the only candidates in the event satisfy muon-related L0 selections (exclusive TOS, xTOS, as it is required they are TOS and that do not belong to TIS). At the HLT stage, the trigger decision must be caused by the signal muon candidates. The analysis is run simultaneously on the two trigger categories, labelled TIS and xTOS in reference to the L0 decision, hereafter referred to as trigger categories. By adding the category of events that are triggered independently of the signal, the trigger efficiency is doubled.

3. Strategy and signal selection

This measurement benefits from both the large K^0_{S} and K^0_{L} production cross-sections at the LHC (around 1 K^0_{S} or K^0_{L} is produced per event [13]), as well as the forward production of kaons which fall within the LHCb detector acceptance. Candidates of $K^0_{\mathrm{S}} \to \mu^+\mu^-\mu^+\mu^-$ decays are reconstructed from two pairs of muons with opposite charge, forming a sufficiently-detached

secondary vertex with an invariant mass lower than $600\,\mathrm{MeV/c^2}$. A blinding procedure is followed: selected candidates in the four-muon invariant-mass region $490 < m_{4\mu} < 510\,\mathrm{MeV/c^2}$, which, estimated from simulation, contains $\approx 97\%$ of the signal, are removed from the data sample until the analysis procedure is finalized.

The branching fraction is measured relatively to that of $K^0_S \to \pi^+\pi^-$ [14], which allows to compute the branching fractions without knowledge of the total number of K^0 produced at PV. This decay is chosen as the normalisation channel because of its large BF and similar kinematics. The $K^0_S \to \pi^+\pi^-$ decay candidates are reconstructed from trigger-unbiased data selected by a prescaled trigger with minimal requirements ensuring some event activity. The K^0_S from both the signal and the normalisation channel are required to come from the PV. Simulation is used to model the effects of the detector acceptance and selection requirements.

Having the same final state and the decay topology makes it difficult to disentangle $K^0_L \to \mu^+\mu^-\mu^+\mu^-$ decays from $K^0_S \to \mu^+\mu^-\mu^+\mu^-$ decays. For this reason, $K^0_L \to \mu^+\mu^-\mu^+\mu^-$ decays are neglected when setting an upper limit on $\mathcal{B}(K^0_S \to \mu^+\mu^-\mu^+\mu^-)$, and vice versa. This approach yields conservative upper limits in the presence of signal. If a signal was observed, it would be identified as $K^0_{S(L)} \to \mu^+\mu^-\mu^+\mu^-$, without specifying the K^0 mass eigenstate.

Background contributions to the signal channel are reduced via a combination of cuts on several variables. Requirements on the track quality, track χ^2_{IP} (defined as the difference in the vertex-fit χ^2 of a given PV reconstructed with and without the track being considered), and particle identification (PID) of the muons are set for both the signal and normalisation channels. An additional cut on the variables from the Armenteros-Podolanski plane [15] on the normalisation channel is applied to reduce contributions from $\Lambda^0 \to p\pi^-$ decays.

The dominant background source in the signal channel arises from random combinations of tracks originating near a pp interaction region or from inelastic collisions with the detector material. A Boosted Decision Tree (BDT) classifier [16, 17] is trained to significantly reduce these contributions. One BDT is trained per trigger category, using as input variables the significance of the distance from the candidate decay vertex to the detector [18], the smallest impact parameter (IP, defined as the minimum distance of the track to PV) of each of the four muon candidates with respect to any of the PVs reconstructed in the event, the smallest IP of the K^0_S candidates to any of the PVs reconstructed in the event, the transverse distance of the K^0_S candidate to the beam line, the maximum distance of closest approach between the four final-state tracks, and the minimum angle between each pair of muons.

The BDT is trained with simulated $K^0_S \to \mu^+\mu^-\mu^+\mu^-$ decays as a proxy for signal, and $K^0_S \to \mu^+\mu^-\mu^+\mu^-$ candidates from the invariant-mass sidebands in data, which cover $450 < m_{4\mu} < 490\,\mathrm{MeV/c^2}$ and $510 < m_{4\mu} < 600\,\mathrm{MeV/c^2}$, as a proxy for background.

The BDT requirement is optimized for the best expected limit at a 90% confidence level (C.L.) using simulated pseudo-experiments. The signal efficiency of the BDT requirement is approximately 80% while rejecting almost all the background candidates. After the BDT cut, only one candidate per event is kept, which is chosen randomly.

4. Normalisation and invariant-mass fit

Given the use of a normalisation channel, as mentioned above, the signal yield, N_{sig}, is translated to a branching fraction as

$$\mathcal{B}(K^0_{S(L)} \to \mu^+\mu^-\mu^+\mu^-) \equiv \alpha N_{\mathrm{sig}}. \tag{3}$$

where the factor α, or single event sensitivity, is calculated as

$$\alpha_{K^0_S(K^0_L)} = \mathcal{B}(K^0_S \to \pi^+\pi^-) \times \frac{s_{\mathrm{MB}}}{N_{\mathrm{norm}}} \times \frac{\varepsilon_{\mathrm{norm}}}{\varepsilon_{\mathrm{sig}}} \approx 2.10 \times 10^{-12}(9.54 \times 10^{-10}). \tag{4}$$

Here, $\varepsilon_{\mathrm{norm}}(\varepsilon_{\mathrm{sig}})$ represents the full selection efficiencies of $K^0_S \to \pi^+\pi^-$ ($K^0_{S(L)} \to \mu^+\mu^-\mu^+\mu^-$) candidates, corrected for data-simulation differences. In particular, the track reconstruction

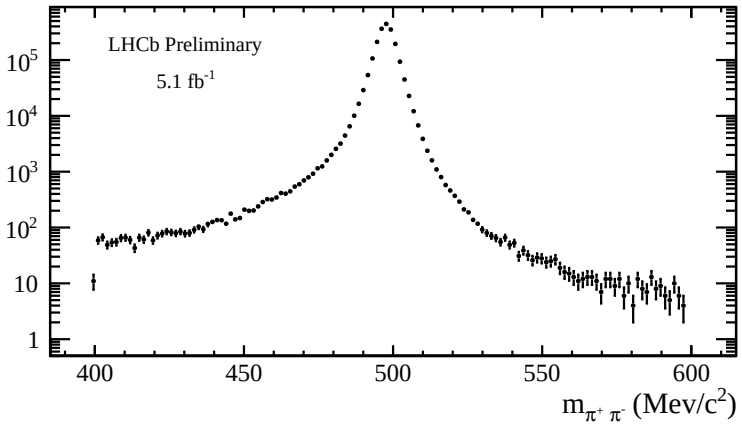

Figure 2. Invariant-mass distribution for the $K^0_S \to \pi^+\pi^-$ selected candidates in the full dataset.

and particle identification efficiencies are corrected. The observed number of $K^0_S \to \pi^+\pi^-$ decays in the minimum bias sample is $N_{\rm norm}$, $\mathcal{B}(K^0_S \to \pi^+\pi^-)$ is the branching fraction of the normalisation channel, fixed to $(69.20 \pm 0.05)\%$ [14], and $s_{\rm MB}$ is the prescale factor of the minimum bias trigger averaged over the different data files, weighted by integrated luminosity. Figure 2 shows the invariant-mass distribution of the $K^0_S \to \pi^+\pi^-$ candidates.

The signal yield, $N_{\rm sig}$, is obtained from a maximum likelihood fit to the four-muon invariant-mass distribution of the signal candidates in the two trigger categories, where the background events are assumed to follow an exponential function and the signal invariant-mass shape is parameterized using a Hypatia distribution [19]. The invariant-mass distributions of the selected candidate events are shown in Fig. 3. The parameter values of the signal distribution are obtained from simulated events with data-driven corrections obtained from $K^0_S \to \pi^+\pi^-$ decays. Gaussian constraints accounting for the systematic uncertainties in (4), are incorporated into the fit. The largest uncertainties are assigned to the trigger selection, as the efficiencies of the TIS (xTOS) category are known to 10(21)% at the L0 leval and 11% at the HLT1 level.

Upper limits for both branching fractions are calculated before unblinding by integrating the profile likelihood from the positive side of the branching fraction. After unblinding, no events are observed in the signal mass window of either sample, leading to an upper limit of

$$\mathcal{B}(K^0_{S(L)} \to \mu^+\mu^-\mu^+\mu^-) < 5.1 \times 10^{-12}\ (2.3 \times 10^{-9}) \text{ at } 90\% \text{ C.L.}$$

5. Future prospects and conclusions

The LHCb upgrade takes place over two phases. By the end of Upgrade I, which covers Run 3 (2022-2024) and Run 4 (2028-2030), an integrated luminosity of around $50\,\text{fb}^{-1}$ is expected to be reached [20]. That number is expected to go up to $300\,\text{fb}^{-1}$ after the Upgrade II is done. This will include Run 5 (2032-2034) and Run 6 (2036-2040). Run 3, currently in progress, is removing the hardware trigger step, with only software trigger selections being applied for the new collected data, leading up to an increase in the trigger efficiency.

For an integrated luminosity of around $50\,\text{fb}^{-1}$ (Upgrade I), a full order of magnitude is expected to be gained for the probing scale of the branching fractions of $K^0_{S(L)} \to \mu^+\mu^-\mu^+\mu^-$, which means that sensitivities allowed by the aforementioned dark photons models will be reached. In Fig. 4, an extrapolation of the results obtained in the analysis described in these proceedings to the luminosities expected for the LHCb upgrade, is presented. It also shows that

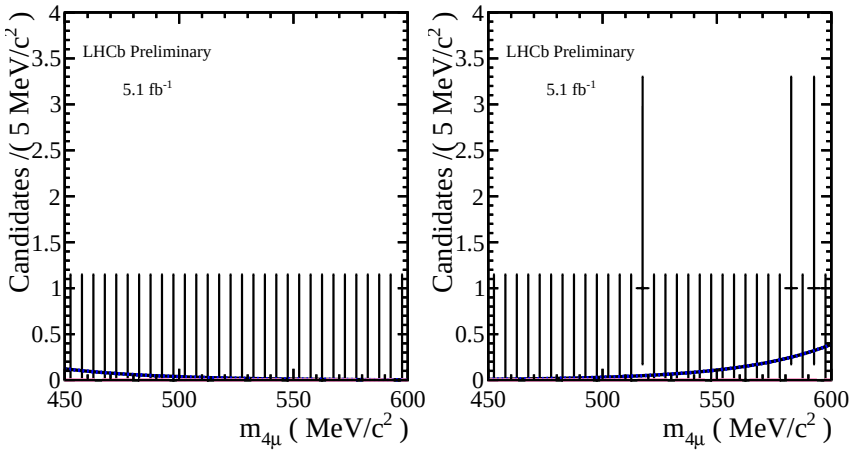

Figure 3. Invariant-mass distribution of the observed $K^0_S \to \mu^+\mu^-\mu^+\mu^-$ candidates in the (left) xTOS trigger category, and (right) TIS trigger category. The blue lines represent the simultaneous fit to both categories, using the exponential functions to represent the background.

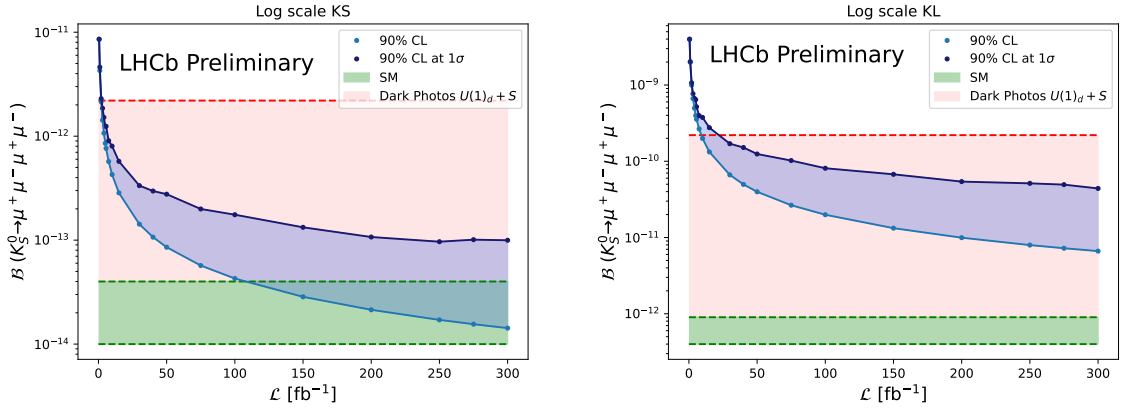

Figure 4. Extrapolation of the expected sensitivities to the data sizes that are planned to be collected by the LHCb experiment

another order of magnitde will be gained after Upgrade II, and the detector could be reaching sensitivities at the level of the SM prediction for $\mathcal{B}(K^0_S \to \mu^+\mu^-\mu^+\mu^-)$.

Also on LHCb's horizons are the studies of di-electron modes, including $K^0_S \to e^+e^-e^+e^-$ and $K^0_S \to \mu^+\mu^-e^+e^-$, normalising to the known $K^0_S \to \pi^+\pi^-e^+e^-$ mode. However, low-momentum electrons are challenging to reconstruct and trigger on, limiting the sensitivity with respect to the 4-muonic channel.

To conclude, these proceedings have presented a search for $K^0_{S(L)} \to \mu^+\mu^-\mu^+\mu^-$ analysing $5.1\,\text{fb}^{-1}$ of LHCb data recorded from 2016 to 2018. No signal was observed, with the obtained upper limits being the first reported for the $K^0_{S(L)} \to \mu^+\mu^-\mu^+\mu^-$ decay modes. The observed values are very close to the maximum values allowed in the dark photon models [2].

References

[1] D'Ambrosio G, Greynat D and Vulvert G 2013 *Eur. Phys. J. C* **73** 2678 (*Preprint* 1309.5736)
[2] Goudzovski E *et al.* 2022 (*Preprint* 2201.07805)

[3] Hostert M and Pospelov M 2022 *Phys. Rev. D* **105** 015017 (*Preprint* 2012.02142)
[4] Aaij R *et al.* (LHCb collaboration) 2013 *JHEP* **01** 090 (*Preprint* 1209.4029)
[5] Aaij R *et al.* (LHCb collaboration) 2020 *Phys. Rev. Lett.* **125** 1231801 (*Preprint* **2001.10354**)
[6] Alves Jr A A *et al.* (LHCb collaboration) 2008 *JINST* **3** S08005
[7] Aaij R *et al.* (LHCb collaboration) 2015 *Int. J. Mod. Phys.* **A30** 1530022 (*Preprint* 1412.6352)
[8] Aaij R *et al.* 2014 *JINST* **9** P09007 (*Preprint* 1405.7808)
[9] Adinolfi M *et al.* 2013 *Eur. Phys. J. C* **73** 2431 (*Preprint* 1211.6759)
[10] d'Argent P *et al.* 2017 *JINST* **9** P11016 (*Preprint* 1708.00819)
[11] Alves Jr A A *et al.* (LHCb Collaboration) 2013 *JINST* **8** P02022 (*Preprint* 1211.1346)
[12] Aaij R *et al.* 2013 *JINST* **8** P04022 (*Preprint* 1211.3055)
[13] Alves Junior A A *et al.* 2019 *JHEP* **05** 048 (*Preprint* 1808.03477)
[14] Workman R L *et al.* (Particle Data Group) 2022 *Prog. Theor. Exp. Phys.* **2022** 083C01
[15] Podolanski J and Armenteros R 1954 *The London, Edinburgh, and Dublin Philosophical Magazine and Journal of Science* **45** 13–30 URL https://doi.org/10.1080/14786440108520416
[16] Breiman L, Friedman J H, Olshen R A and Stone C J 1984 *Classification and regression trees* (Belmont, California, USA: Wadsworth international group)
[17] Freund Y and Schapire R E 1997 *J. Comput. Syst. Sci.* **55** 119
[18] Alexander M *et al.* 2018 *JINST* **13** P06008 (*Preprint* 1803.07466)
[19] Martínez Santos D and Dupertuis F 2014 *Nucl. Instrum. Meth.* **A764** 150–155 (*Preprint* 1312.5000)
[20] LHCb collaboration 2020 CERN-LHCC-2020-006 URL http://cds.cern.ch/record/2717938